THE JOURNAL OF BIOLOGICAL CHEMISTRY VOL. 282, NO. 19, pp. 14226–14237, May 11, 2007

A Mutant αII-spectrin Designed to Resist Calpain and Caspase Cleavage Questions the Functional Importance of This Process *in Vivo*[*]

Received for publication, January 2, 2007, and in revised form, February 20, 2007 Published, JBC Papers in Press, March 20, 2007, DOI 10.1074/jbc.M700028200

Fleur Meary[‡§¶], Sylvain Metral[‡§¶], Chrystophe Ferreira[‖], Dominique Eladari[‡‡], Yves Colin[‡§¶], Marie-Christine Lecomte[‡§¶], and Gaël Nicolas[‡§¶1]**

From the [‡]INSERM, U665, Paris F-75015, [§]Institut National de la Transfusion Sanguine, Paris F-75015, [¶]Université Paris 7/Denis Diderot, Paris, F-75005, [‖]Institut Fédératif de Recherche Claude Bernard, Faculté de Médecine Xavier Bichat, Paris F-75018, [**]INSERM, U652, Paris F-75006, and [‡‡]Université Paris Descartes, Faculté de Médecine René Descartes, and AP-HP, Département de Physiologie de l'Hôpital Necker-Enfants Malades, Paris F-75006, France

α- and β-spectrins are components of molecular scaffolds located under the lipid bilayer and named membrane skeletons. Disruption of these scaffolds through mutations in spectrins demonstrated that they are involved in the membrane localization or the maintenance of proteins associated with them. The ubiquitous αII-spectrin chain bears in its central region a unique domain that is sensitive to several proteases such as calpains or caspases. The conservation of this region in vertebrates suggests that the proteolysis of αII-spectrin by these enzymes could be involved in important functions. To assess the role of αII-spectrin cleavage *in vivo*, we generated a murine model in which the exons encoding the region defining this cleavage sensitivity were disrupted by gene targeting. Surprisingly, homozygous mice expressing this mutant αII-spectrin appeared healthy, bred normally, and had no histological anomaly. Remarkably, the mutant αII-spectrin assembles correctly into the membrane skeleton, thus challenging the notion that this region is required for the stable biogenesis of the membrane skeleton in nonerythroid cells. Our finding also argues against a critical role of this particular αII-spectrin cleavage in either major cellular functions or in normal development.

Spectrin was first identified at the inner surface of the red blood cell membrane and is well known to be the central component of the membrane skeleton, a ubiquitous and complex spectrin-actin scaffold. Spectrins are long and flexible molecules composed of two subunits, α and β, that intertwine to form α/β heterodimers. Spectrin is subsequently integrated into the membrane skeleton as $(\alpha/\beta)_2$ tetramers resulting from the self-association of α/β heterodimers (1). These tetramers constitute the filaments of the lattice, the nodes of which are cross-linked by short actin filaments (2). Each spectrin subunit is mainly composed of a succession of triple helical repeats. The spectrin-based membrane skeleton is responsible for the characteristic shape and the unique physical properties of red blood cells, such as deformability and remarkable stability to shear stress. Defects in components of this network lead to membrane fragility and are associated with various hemolytic anemias (3).

This membrane skeleton network was identified in all nonerythroid mammalian cells with components, including spectrins, that are very similar to those found into red blood cells but in most cases are expressed by different genes. There are only two genes encoding α-spectrins. The αI-spectrin is mainly expressed into red blood cells in association with βI. The ubiquitous αII-spectrin (also named α-fodrin) is actually considered as the major α-spectrin expressed in nonerythroid cells, and the αII/βII heterodimers are the main species described in these cells. Disruption of membrane skeletons through β-spectrin mutations was found to be responsible for the abnormal localization or the maintenance of proteins associated with spectrin-based complexes (4–7).

There are no mammalian models describing αII-spectrin mutations. Defects in the unique α-spectrin ortholog to the αII-gene from vertebrates are lethal in larva in *Drosophila melanogaster* and *Caenorhabditis elegans*, arguing for the crucial role of the entire protein (8–10).

αII-spectrin differs from the erythroid αI-spectrin mainly in one feature as follows: the presence of a short region consisting of 36 amino acids encoded by three exons and located in the middle part of the protein near an SH3[2] domain. This region bears several cleavage sites for different proteases, including calpains and caspases. Moreover, it contains a binding site for calmodulin, and a calmodulin/αII-spectrin interaction was shown to regulate the cleavage by calpains and caspases (11). We and others found that calpain cleavage is also regulated by phospho/dephosphorylation of the tyrosine residue (position 1176) located in the calpain recognition site (12, 13). More recently, it was shown that this region here named CCC (for calpain, caspase, calmodulin) is also targeted by proteases (*e.g.* Pet) secreted by pathological enteroaggregative strains of *Escherichia coli* (14, 15).

* This work was supported by INSERM and by the Institut National de la Transfusion Sanguine. The project was initiated at unit 409 of INSERM. The costs of publication of this article were defrayed in part by the payment of page charges. This article must therefore be hereby marked "*advertisement*" in accordance with 18 U.S.C. Section 1734 solely to indicate this fact.

[1] To whom correspondence should be addressed: INSERM U665, Institut National de la Transfusion Sanguine, 6 Rue Alexandre Cabanel, Paris F-75015, France. Tel.: 33-1-44-49-30-00 (ext. 32-02); Fax: 33-1-43-06-50-19; E-mail: gnicolas@idf.inserm.fr.

[2] The abbreviations used are: SH, Src homology; CHAPS, 3-[(3-cholamidopropyl)dimethylammonio]-1-propanesulfonic acid; PBS, phosphate-buffered saline; BSA, bovine serum albumin; BDP, breakdown product; MEF, murine embryonic fibroblast; PGK, phosphoglycerate kinase; ES, embryonic stem; ALLN, *N*-acetyl-Leu-Leu-norleucinal.

Our working hypothesis is that specific proteolysis of αII-spectrin by proteases such as calpains and caspases could be a pathway for local and global membrane skeleton reorganization that occurs during different cellular mechanisms such as cell shape regulation, cell differentiation, motility, or cytokinesis (16). As an example, cells treated with the Pet protease underwent actin remodeling, which might be the consequence of αII-spectrin cutting (15). Cleavage by calpains could be more physiological than cutting by caspases, which are mainly activated during the irreversible apoptotic process. However, calpains can also be overactivated in pathological conditions (17). It has been proposed that the αII-spectrin cleavage during apoptosis can be responsible for the membrane blebbing, which is typical in this process.

To address *in vivo* the role of the CCC αII-spectrin region, we generated mice in which this region is deleted by using gene targeting. This is the first report concerning the description of a murine mutant for αII-spectrin. Surprisingly, homozygous mice expressing this mutant spectrin are healthy, breed normally, and present no histological anomaly, arguing against the role of this particular αII-spectrin cleavage in either major cellular functions or in normal development.

MATERIALS AND METHODS

Construction of the Targeting Vector—Both *Spna1* and *Spna2* genes encoding αI- and αII-spectrin, respectively, have similar intron-exon organizations. The main difference consists in the presence of three additional exons in the *Spna2* gene, which encode the specific CCC region of αII-spectrin (Fig. 1). The first exon (24 bp), which we arbitrarily named exon "24b" (to respect the nomenclature of other exons based on intron-exon organization of *Spna1* gene), encodes an 8-amino acid sequence containing the calpain cleavage site. The two following exons, exons "24c" (36 bp) and "24d" (48 bp), encode the caspase cleavage site and the calmodulin binding domain, respectively. We also named "Σ1" for the alternative spliced exon located between exons 22 and 23, which encodes a 20-amino acid sequence specific for the αIIΣ1 isoform. Our strategy consists of the elimination of these three exons using a classical knock-out approach. However, the rest of the encoded mutant αII-spectrin was kept intact as the deletion should not impair the translation reading frame.

To evaluate the splicing of the chimeric intron resulting from Cre recombination, a minigene model was developed. A genomic DNA portion of the murine *Spna2* gene, including exon 24, chimeric intron 24/24d, and exon 25, was cloned into pcDNA3 plasmid (Invitrogen). After transfection of this construct into NIH-3T3 fibroblastic cells, we demonstrated that this chimeric intron was correctly spliced using reverse transcription-PCR (data not shown).

The targeted mutation was introduced at the *Spna2* locus by homologous recombination in embryonic stem (ES) cells. The targeting construct was assembled as follows. All amplifications were performed with *Pfx* DNA polymerase (Invitrogen). All primers were from Invitrogen or MWG Biotec. Genomic DNA (129/Sv) was amplified using primers 5′-cagtcagcctcgagggagaacc-3′ and 5′-gggggatccaaccaagggcaccacagacac-3′, and the 3.5-kbp amplified product was cloned into XhoI-BamHI-linearized pBluescript II KS plasmid (Stratagene). The resulting plasmid was linearized with BamHI and NotI, and a 3.6-kbp fragment amplified with primers 5′-gggggatccttaagttcctaagttccttaaatagataagtgttttg-3′ and 5′-ataagaatgcggccgcataacttcgtatagcatacattatacgaagttatttgaatacttggtccccttggga-3′ (LoxP site is underlined) was subcloned (after digestion with BamHI and NotI). The resulting plasmid was linearized with NotI and SacII and a 3.5-kbp fragment amplified with primers 5′-gggggatccataacttcgtataatgtatgctatacgaagttatgcggccgcacatgagcctatgggagtcattctc-3′ (LoxP site is underlined) and 5′-tccccgcggctcgagacctgtcaagtcatgaagccccagtc-3′ was subcloned (after digestion with NotI and SacII). The resulting plasmid was linearized with BamHI to receive a 2.1-kbp "floxed" PGK promoter/hygromycin resistance cassette (a generous gift from Marco Giovannini, INSERM U434, Paris, France). Orientation of the cassette was checked. Each cloned fragment was completely sequenced at each step. No mutation was found when compared with sequences from data bases. The 12.7-kbp recombination fragment was separated from pBluescript II KS backbone using XhoI digestion, agarose electrophoresis, gel purification QIAquick PCR purification kit, Qiagen), and then a second purification (QIAquick PCR purification kit, Qiagen).

Gene Targeting in ES Cells and Generation of Chimeras—Following linearization at the XhoI site, the 12.7-kbp targeting vector was electroporated into 129/Sv-ter ES cells grown on feeder layers (Mouse Clinical Institute, Illkirch, France). After hygromycin selection (150 μg/ml), DNA of resistant clones was analyzed by Southern blot and PCR strategies to identify correctly targeted ES cells. To generate chimeras, targeted ES cells were injected into C57BL/6J host blastocysts that were transferred into foster females. Male chimeras were selected by coat color and crossed with C57BL/6J females to obtain germ line transmission of the targeted *Spna*2 allele. Males chimeras were then bred with 129/Sv-ter females in order to put the targeted allele on a homogeneous 129/Sv genetic background. The Cre recombination was performed by crossing mice bearing the targeted *Spna2* allele with the MeuCre40 transgenic line (18). Recombined alleles were then segregated by crossing the mosaic mice with 129/Sv mice (Charles River Laboratories). In this study we focused only on the allele that recombined between the LoxP site 1 and LoxP site 3 (see Fig. 1). All experiments were performed in compliance with French laws on animal care, using relevant INSERM guidelines.

Genotype Analysis—Genotyping on mouse DNA was performed using Southern blot (data not shown, available upon request) or by using a multiplex PCR to identify wild-type and *Spna2* knock-out alleles. Genomic DNA (0.1–0.5 μg) was used in a 25-μl reaction that included five primers as follows: primer 1, 5′-gatctgaaagccaatgagtctcggc-3′ (forward, annealing in exon 24); primer 2, 5′-tacatagagaatggccagtcttttgac-3′ (forward, annealing in intron 24d), primer 3, 5′-gcacaactgggtaaggttcctattcc-3′ (reverse, annealing in intron 24d), primer 4, 5′-cccggcattctgcacgcttc-3′ (forward, annealing in PGK*hygro* cassette) and primer 5- 5′ tccatggcctccgcgaccg 3′ (reverse, annealing in PGK*hygro* cassette). The wild-type *Spna2*^{S} allele amplifies a single amplicon (201 bp with primers 2 + 3, see Fig. 2*A*); the targeted *Spna2* allele amplifies two amplicons (243 bp with primers 2 + 3 and 450 bp with primers 4 + 5), and the Cre

recombined (LoxP site 1 with LoxP site 3) *Spna2*^{R} allele amplifies one single amplicon (374 bp with primers 1 + 3, see Fig. 2*A*). PCR was performed as follows: 35 cycles (each cycle consisting of 20 s at 94 °C, 20 s at 65 °C, and 30 s at 72 °C) with an initial denaturation at 94 °C for 4 min, and a final elongation at 72 °C for 5 min in 20 mM Tris-HCl (pH 8.4), 50 mM KCl, 2 mM $MgCl_2$, 0.2 mM each dNTP, 0.18 mM each primer 1–3, 0.2 mM each primer 4–5, 0.5 unit of Taq polymerase (Invitrogen). The reaction was analyzed on 2% agarose gel containing SYBR Safe (Invitrogen). This PCR method for genotyping gave the same results as Southern blot (data not shown). Cre transgene genotyping was performed as described (19).

Reverse Transcription—Total RNA was extracted from organs biopsies with RNA PLUS™ (Q-Biogen). The cDNA synthesis was performed in 20 μl with 2 μg of total RNA, in the presence of 0.5 mM of each dNTP, 10 ng/μl of random hexanucleotide primers, 0.1 mg/ml bovine serum albumin (BSA), 1 unit/μl RNase OUT (Invitrogen), 10 mM dithiothreitol, and 10 units/μl SuperScript™ reverse transcriptase (Invitrogen). The reaction was conducted for 65 min at 42 °C before reverse transcriptase was inactivated for 6 min at 96 °C. After reaction, cDNA was diluted with 80 μl of 10 mM Tris-HCl, 0.1 mM EDTA (pH 8.0). PCR amplification was performed with 2.5 μl of reverse transcriptase reaction mixture in 25 μl of 20 mM Tris-HCl (pH 8.4), 50 mM KCl, 2 mM $MgCl_2$, 0.2 mM each dNTP, 0.2 mM each primer as follows: forward, 5′-gggaagcttccaccatggatctgaaagccaatgagtctcggc-3′ (annealing in exon 24), and reverse, 5′-gggctcgaggtgaaacctctgtacttcgtgtgcac-3′ (annealing in exon 25), 0.5 units of *Taq* polymerase (Invitrogen). PCR was performed as follows: 30 cycles (each cycle consisting of 20 s at 94 °C, 20 s at 60 °C, and 40 s at 72 °C) with an initial denaturation step at 94 °C for 5 min, and a final elongation step at 72 °C for 5 min. The reaction was analyzed on 1.5% agarose gel containing SYBR Safe (Invitrogen).

Primary Murine Embryonic Fibroblasts (MEFs)—Primary fibroblast cultures were established from E13.5 embryos. The time of fertilization was determined by observation of copulation plugs, and noon of that day was defined as E0.5. Embryos were dissected from pregnant mutant (*Spna2*$^{R/R}$) females that had been bred with mutant males or from wild-type females (*Spna2*$^{S/S}$) that had been bred with wild-type males. The yolk sacs, heads, and internal organs were removed. Carcasses were carefully rinsed with D-PBS (Invitrogen), cut into very small pieces with fine scissors, and treated with trypsin/EDTA (Invitrogen; 4 ml per embryo) for 5 min at 37 °C under agitation. Clumps of cells were disrupted by repeated aspirations through a 5-ml pipette. The trypsin was neutralized by adding an equal volume of culture medium (Dulbecco's modified Eagle's medium (4.5 g/liter glucose, 110 mg/liter pyruvate sodium, 862 mg/liter GlutaMAX™ I) supplemented with 10% fetal bovine serum and antibiotics (100 units/ml penicillin and 100 μg/ml streptomycin). After centrifugation, the cells were resuspended in culture medium and plated onto 10-cm plates. Fibroblasts were maintained at 37 °C under 5% CO_2. Cells were diluted at a 1:5 ratio 24 h later on new plates, and confluence was obtained 3 days later. They were frozen in 90% fetal bovine serum with 10% Me_2SO. Cells were passed every three or 4 days. We observed a growth crisis after passage 5 (approximately 2 weeks), so the study presented here was only performed with fibroblasts maintained at passage 4 maximum. When indicated, cells were preincubated with 5 μM calpain inhibitor I (*N*-acetyl-Leu-Leu-norleucinal (ALLN); BioMol).

Induction of Apoptosis—Apoptosis was triggered using either 1 mM H_2O_2 during 24 h in Dulbecco's modified Eagle's medium supplemented with 10% FBS or UV irradiation (312 nm) for 5 min. The UV irradiation was delivered by six bulbs (15 watts, T15M) on a 35 × 20 cm surface.

Caspase and Calpain Cleavage Assay—Organs were submitted to an Ultraturrax rotor in the following ice-cold lysis buffer: 50 mM Hepes buffer (pH 7.5), 150 mM NaCl, 1.5 mM $MgCl_2$, 1 mM EDTA, 10% glycerol, 1% Triton, 2 mM 4-(2-aminoethyl) benzenesulfonyl fluoride, 20 μg/ml pepstatin, 10 μg/ml bestatin. For post-mortem analysis, pieces of liver were kept at 4 °C for 48 h and were then treated as the other organs. Triton-soluble extracts correspond to the supernatant obtained after centrifugation at 13,000 rpm (Eppendorf 5415R Centrifuge) for 20 min (4 °C) of the lysed organs previously kept on ice for 20 min. The pellets were further solubilized in the same lysis buffer containing 1% SDS and kept on ice for 20 min; insoluble extracts correspond to the supernatant obtained after centrifugation at 13,000 rpm for 20 min (4 °C) of these resuspended pellets. Extracts from MEF culture were obtained in a similar way except that samples were vigorously vortexed instead of treatment with the Ultraturrax rotor. Protein concentration was measured using the micro-BC assay protein quantification kit (Uptima) with bovine serum albumin (62.5 to 2000 ng) as standard samples. Wild-type or mutant endogenous αII-spectrin present in Triton-soluble cell lysates were submitted to exogenous recombinant proteases. Recombinant caspase 2 (catalog number SE-175, Biomol) and caspase 3 (catalog number 235417, Calbiochem, or catalog number C-1305, A. G. Scientific) were used at 1.5–1.7 units/μl of reaction in 10 mM dithiothreitol, 100 mM NaCl, 0.1% (v/v) CHAPS, and 50 mM Hepes buffer (pH 7.4) (final volume, 60 μl) for 2 (caspase 2) or 2–4 h (caspase 3) at 30 °C. Digestion with μ-calpains (catalog number C6108, Sigma) was used with 3.2 units/μl of reaction in 50 mM Tris-HCl buffer (pH 7.5), 150 mM NaCl, 2 mM $MgCl_2$, 100 nM recombinant calmodulin for 1 h at 30 °C (final volume, 60 μl). Cleavage reactions were stopped by addition of electrophoresis sample buffer, and the proteins were analyzed by Western blot.

Western Blotting—Samples were analyzed by SDS-PAGE (7% polyacrylamide gel) and transferred onto nitrocellulose membrane (Optitran®, Schleicher & Schuell) using a Tris/glycine buffer (Bio-Rad). After saturation in 10 mM phosphate buffer (pH 7.5), 150 mM NaCl, 0.05% Tween 20 (PBST), and 5% (w/v) nonfat-milk, blots were probed with specific antibodies. Antibodies used are as follows: immunopurified anti-SH3 domain of αII-spectrin (10 ng/ml (12)); anti-αII-spectrin monoclonal antibody (50 ng/ml, FG 6090 antibody, clone AA6; BioHit); immunopurified anti-CCC region obtained by immunization of rabbits against the NH_2-Cys-Ser-Lys-Thr-Ala-Ser-Pro-Trp-Lys-Ser-Ala-Arg-Leu-Met-Val-His-Thr-Val-Ala-Thr-Phe-Asn-Ser-Ile-Lys-COOH peptide coupled to keyhole limpet hemocyanin (1:500 dilution; Covalab). The antibodies against the mutant αII-spectrin were obtained by immunization of rab-

TABLE 1

K_a/K_s values of the CCC region

Alignment of the nucleotide and amino acid (in black) sequences of exons 24b, 24c, and 24d of αII-spectrin from various species. Hs, *H. sapiens*; Pt, *P. troglodytes*; Mm, *M. musculus*; Rn, *R. norvegicus*; Bt, *B. taurus*; Cf, *C. familiaris*, and Gg, *G. gallus*. Changes in nucleotides or amino acids (compared to the human sequences) are indicated in gray.

```
     <          exon 24b          > <                exon 24c                >
Hs- gaa gtg tat ggc atg atg ccc agg gat gaa act gat tcc aag aca gcc tcc ccg tgg aag
Hs- E   V   Y   G   M   M   P   R   D   E   T   D   S   K   T   A   S   P   W   K

Pt- gaa gtg tat ggc atg atg ccc agg gat gaa act gat tcc aag aca gcc tcc ccg tgg aag
Pt- E   V   Y   G   M   M   P   R   D   E   T   D   S   K   T   A   S   P   W   K

Mm- gag gtg tat ggt gcg atg ccc agg gat gaa gca gat tcc aag acg gcc tcc cca tgg aag
Mm- E   V   Y   G   A   M   P   R   D   E   A   D   S   K   T   A   S   P   W   K

Rn- gag gtg tat ggt atg atg ccc agg gat gaa gca gat tcc aag acc gcc tcc cca tgg aag
Rn- E   V   Y   G   M   M   P   R   D   E   A   D   S   K   T   A   S   P   W   K

Bt- gag gtg tat ggc gcg atg ccc agg gat gaa tct gat tcc aag aca gcc tcc cct tgg aag
Bt- E   V   Y   G   A   M   P   R   D   E   S   D   S   K   T   A   S   P   W   K

Cf- gag gtg tat ggc atg atg ccc agg gat gac acg gat tcc aag act gca tcc cct tgg aag
Cf- E   V   Y   G   M   M   P   R   D   D   T   D   S   K   T   A   S   P   W   K

Gg- gaa gtc tat gga atg atg ccc aga gat gaa act gat tct aag aca gcc tct cct tgg aag
Gg- E   V   Y   G   M   M   P   R   D   E   T   D   S   K   T   A   S   P   W   K


     <                          exon 24d                          >
Hs- tct gct cgt ctg atg gtt cac acc gtg gcc acc ttt aat tcc atc aag
Hs- S   A   R   L   M   V   H   T   V   A   T   F   N   S   I   K

Pt- tct gct cgt ctg atg gtt cac acc gtg gcc acc ttt aat tcc atc aag
Pt- S   A   R   L   M   V   H   T   V   A   T   F   N   S   I   K

Mm- tct gct cga ctg atg gtc cat aca gtg gct acc ttc aac tcc atc aag
Mm- S   A   R   L   M   V   H   T   V   A   T   F   N   S   I   K

Rn- tct gct cga ctg atg gtc cac aca gtg gcc acc ttc aac tcc atc aag
Rn- S   A   R   L   M   V   H   T   V   A   T   F   N   S   I   K

Bt- tct gct cgc ctg atg gtt cac acc gtg gcc acc ttt aat tcc atc aag
Bt- S   A   R   L   M   V   H   T   V   A   T   F   N   S   I   K

Cf- tct gct cgt ctg atg gtt cat acc gtg gcc acc ttt aat tcc atc aag
Cf- S   A   R   L   M   V   H   T   V   A   T   F   N   S   I   K

Cg- tct gca cgt atg atg gta cac aca gtg gca acg ttt aac tca atc aag
Cg- S   A   R   M   M   V   H   T   V   A   T   F   N   S   I   K
```

bits with NH_2-Ala-Val-Gln-Gln-Gln-Glu-Leu-Asn-Glu-Arg-COOH peptide coupled to keyhole limpet hemocyanin (200 ng/ml; DB-BioRun). Immunopurifications were performed against the immunization peptide or recombinant αII-spectrin peptide with HiTrap column (Amersham Biosciences). Immunocomplexes with immunopurified antibodies against mutant αII-spectrin were performed in 50 mM Tris buffer (pH 7.2), 150 mM NaCl, 10 mM $MgCl_2$, 10 mM $CaCl_2$. Other immunocomplexes were formed in PBST with or without 5% (w/v) nonfat milk. Detections were performed with either anti-rabbit IgG or anti-mouse IgG conjugated with horseradish peroxidase (Nordic Immunological Laboratories) using the Supersignal West Pico chemiluminescence substrate (Pierce) and Gel Doc™ system (Bio-Rad).

Immunohistochemistry on MEF—Cells cultured on glass slides were fixed in 4% paraformaldehyde for 20 min and washed in PBS. Free aldehyde groups were blocked by 50 mM NH_4Cl for 10 min. Slides were washed in PBS, permeabilized in 0.5% Triton for 15 min, and washed again in PBS. To reduce nonspecific binding, slides were incubated in 0.1% PBS/BSA for 15 min. They were then incubated with rabbit polyclonal anti-SH3 αII-spectrin antibody diluted at 2 μg/ml (0.1% PBS/BSA) for 1 h at room temperature. After washings (0.1% PBS/BSA), slides were incubated for 1 h at room temperature with Alexa Fluor™ 488 goat anti-rabbit IgG (1:200 dilution) and Alexa Fluor™ 568 phalloidin (1:50 dilution; Molecular Probes) diluted in 0.1% PBS/BSA. Samples were examined by confocal microscopy using a Nikon Eclipse TE300 inverted microscope equipped with a 60× oil immersion objective NA 1.4 and a D-Eclipse C1 confocal system.

Immunohistochemistry on Tissue Sections—Organs were fixed in 4% formaldehyde (Carlo Erba) in PBS and embedded in paraffin, and 3-μm sections of the paraffin block were deparaffinized with EZ-DeWax™ (BioGenex). Rehydration was com-

TABLE 2

K_a/K_s values of the CCC region

The value of K_a/K_s is calculated and indicated for each couple of vertebrates.

	H. sapiens	*P. troglodytes*	*M. musculus*	*R. norvegicus*	*B. taurus*	*C. familiaris*
P. troglodytes	0					
M. musculus	0.051	0.051				
R. norvegicus	0.022	0.022	0.198			
B. taurus	0.291	0.291	0.020	0.080		
C. familiaris	0.042	0.042	0.080	0.038	0.220	
G. gallus	0.013	0.013	0.029	0.016	0.048	0.012

pleted in demineralized water. Slides were then incubated in 1× Target Retrieval Solution at pH 9.0 (DakoCytomation) and heated for 40 min at 98 °C in a heated water bath. This step unmasked antigen and allowed immunostaining on formaldehyde-fixed paraffin sections, as determined in preliminary experiments (not shown). The tank containing slides was cooled at room temperature for 20 min. To reduce nonspecific binding, sections were rinsed in 0.1% PBS/BSA for 5 min and preincubated for 20 min with antibody diluent with background reducing components (DakoCytomation). The labeling procedure was as follows: affinity-purified anti-SH3 antibodies (4 μg/ml), diluted in antibody diluent with background reducing components, were applied for 1 h at room temperature. After intensive washes with 0.1% PBS/BSA, sections were incubated with a 1:200 dilution (in antibody diluent with background reducing components) of Alexa Fluor® 488 goat anti-rabbit IgG (Molecular Probes) for 30 min at room temperature, followed by washings in 0.1% PBS/BSA. Nuclei were labeled by incubation of 0.2 μg/ml propidium iodide in 0.1% PBS/BSA for 15 min. Sections were mounted with ProLong™ Gold (Molecular Probes) and then examined by confocal microscopy.

We took advantage of the platform present at the Mouse Clinical Institute (Illkirch, France) to perform an extensive histological analysis on mutant males ($n = 3$) or females ($n = 3$) and control wild-type male ($n = 1$) and female mice ($n = 1$). Mice were 6 months old. Organ biopsies analyzed were the salivary glands, pancreas, stomach (trimmed after fixation), duodenum, distal ileum, proximal colon, liver (the median lobe and half of the left lateral lobe), spleen, kidney (trim before fixation), urinary bladder, adrenal glands (both), mesenteric lymph nodes, thoracic aorta, trachea, thyroid gland, esophagus, thymus, heart, entire lung, leg muscle, tongue, white adipose tissue (paragenital fat pad), brown adipose tissue, dorsal tail, footpad and snout skin, eye, Harderian gland, knee joint, brain, and hypophysis. Specific samples from males were preputial gland, right testis and epididymis (fixed in Bouin's fluid), left testis, and epididymis (fixed in neutral buffered formalin), prostate and seminal vesicles. Supplementary samples from females were ovaries, oviducts, vagina, uterus body, uterine horns, and urinary bladder.

K_a/K_s Values—The K_a/K_s value is the ratio of the number of nonsynonymous substitutions per nonsynonymous site (K_a) to the number of synonymous substitutions per synonymous site (K_s), with K_s indicating the background rate of evolution. These parameters allow an estimation of the selective forces acting on a protein sequence during evolution. If a sequence should be kept intact, a K_a/K_s value lower than 1 is expected. The process is called "purifying selection." The K_a/K_s analysis was performed using DnaSP software using cDNA from exons 23 to 27 and protein sequences available from *Homo sapiens*, *Pan troglodytes*, *Mus musculus*, *Rattus norvegicus*, *Bos taurus*, *Canis familiaris*, and *Gallus gallus*.

RESULTS

Analysis of the Selection Pressure on the Central Domain of the αII-spectrin Using the K_A/K_S Evaluation Method—Analysis of the CCC sequences from data bases reveals that this region is highly conserved in vertebrates but does not exist in invertebrates. To estimate the level of constraint on the CCC region, we aligned the orthologous sequences of exon 24b, 24c, and 24d from different species (Tables 1 and 2). Compared with human, the murine sequence (separated by 91 million years (20)) shows 3 nonsynonymous mutations and 12 synonymous mutations in exon 24b, 24c, and 24d with the consequence that there are only two substitutions leading to amino acid change, giving a K_a/K_s

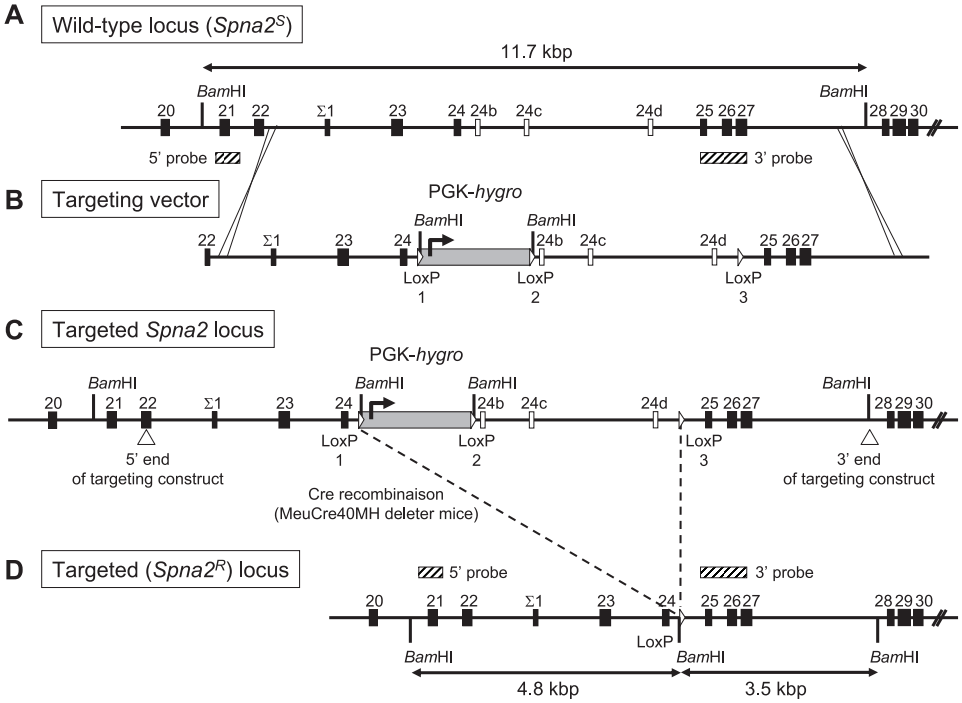

FIGURE 1. **Schematic representation of the genomic structure of the wild-type murine *Spna2*^{S} allele (*A*), the targeting construct (*B*), the targeted *Spna2* allele (*C*), and the *Spna2*^{R} allele between exons 20 and 30 (*D*).** Exons encoding the CCC region are represented by *white boxes*, and other exons are represented by *black boxes*. A floxed PGK-hygromycin cassette (*PGK-hygro*), shown in *gray* (the *arrow* indicates transcriptional orientation), was introduced into intron 24. The LoxP sites are represented by *white arrowheads*. A third LoxP was introduced into intron 24d. BamHI cleavage sites are indicated. The 5′ and 3′ ends of the targeting construct are indicated by *white arrowheads*. The 5′ and 3′ probes are indicated by *hatched boxes*. After recombination with a Cre transgenic line (18), the resulting *Spna2*^{R} allele lacks exons encoding the CCC region and encodes the mutant αII-spectrin.

of 0.051 (Tables 1 and 2). Compared with human, the chicken sequence (separated by 310 million years (20)) shows 1 nonsynonymous mutation and 13 synonymous mutations resulting in only one substitution at the protein level and a K_a/K_s of 0.013. These data reveal that the CCC region is under a strong purifying selection. The pressure to keep intact the protein sequence suggests that the CCC region has at least one important function. It should be noted that the purifying selection is not restricted to the CCC region because K_a/K_s values $\ll 1$ were also found when flanking exons (exon 23 to exon 27) were analyzed.

Generation of Mice—To assess the role of the CCC region and particularly the cleavage of αII-spectrin, we generated a murine model in which the three exons encoding the region were disrupted by gene targeting in embryonic stem cells. The *Spna2* targeting strategy (shown in Fig. 1) introduces two LoxP sites, one upstream of the exon 24b and the other one downstream of the exon 24d allowing the deletion of the exons encoding the CCC region by Cre recombinase. The rest of the encoded mutant αII-spectrin was kept intact as the deletion should not impair the translation reading frame.

Analysis revealed that 20 of 37 hygromycin-resistant ES clones underwent homologous recombination at the *Spna2* locus. Germ line transmission of the mutant allele was achieved with one targeted ES clone in which no additional sites of integration were detected. Chimeric males were crossed with C57BL/6 and 129/Sv females to obtain the targeted *Spna2* allele on C57BL/6–129/Sv mixed or 129/Sv genetic background, respectively. Mice heterozygous for this allele were bred with mice carrying a Cre transgene allowing us to eliminate targeted exons (18). This Cre recombination produces a chimeric intron composed of the upper half of intron 24 and the lower part of intron 24d (Fig. 1*D*). As the resulting allele should produce an αII-spectrin resistant to different proteolytic processes (see below), we named this allele, *Spna2*^{R} (*R* for resistant) in comparison to the wild-type allele, *Spna2*^{S} (*S* for *s*ensitive). Therefore, wild-type mice are named *S/S*, heterozygous mice *S/R*, and homozygous mutant mice *R/R*.

The genotyping shows a mendelian proportion of each genotype on mixed genetic background (containing a contribution of 129/Sv and C57BL/6; Table 3). The homozygous mutant mice ($n = 63$, aged up to 18 months) did not exhibit a particular phenotype and were indistinguishable from heterozygous or wild-type littermates. These animals were healthy and had a normal cage behavior. Furthermore, when interbred, homozygous mutant males and females gave rise to litters that were composed of healthy mice.

We first analyzed this mutation at the RNA level using reverse transcription-PCR and primers located in exons 24 and 25, flanking targeted exons 24b, 24c, and 24d. In homozygous *R/R* mice, we found that liver and kidney expressed a product of the expected size of 221 bp (Fig. 2*B*). Sequencing of this amplicon confirmed the deletion of the three exons and a correct boundary between exon 24 and 25 (Fig. 2*C*), indicating that the chimeric intron resulting from Cre/LoxP recombination between intron 24 and 24d has been correctly spliced. We further analyzed the mutant spectrin at the protein level. We prepared Triton-soluble lysates from organs from mice with different genotypes and analyzed them by Western blotting using different antibodies directed against αII-spectrin. We prepared an antibody directed against the CCC region (from Ser-1186 to Lys-1209). This antibody reveals a protein of the expected size (285 kDa) in samples prepared from wild-type and heterozygous mice (Fig. 2*D*). This antibody does not recognize any band in samples obtained from homozygous mutant mice. We also prepared a specific antibody against the protein junction resulting from fusion of exon 24 with 25. This antibody reveals a protein of the expected size (280 kDa) in heterozygous and homozygous mutants but not in wild-type mice (Fig. 2*D*). As a control, we reprobed blots using either the purified polyclonal antibodies recognizing the αII-spectrin SH3 domain (Fig. 2*D*) or the monoclonal antibody AA6 (data not shown). Both anti-

TABLE 3

Number of mice of each genotype obtained from crossings between *S/R* males and females

Genotypes were determined by PCR at postnatal days 10–12 as described under "Materials and Methods."

	S/S mice	*S/R* mice	*R/R* mice	Total
Pups	23 (27.1%)	42 (49.4%)	20 (23.5%)	85 (100%)

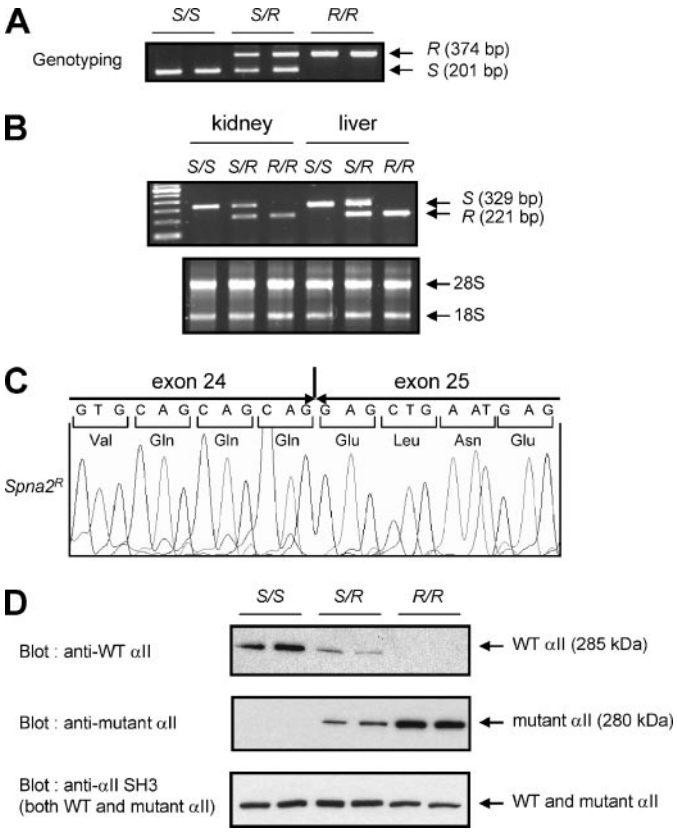

FIGURE 2. **The mutant αII-spectrin is correctly expressed.** *A*, DNA from each genotype (wild-type *S/S*, heterozygous *S/R*, and homozygous *R/R*) was extracted and amplified as described under "Materials and Methods." Amplicons from *Spna2*^{S} (wild-type) allele and *Spna2*^{R} (mutant) allele were 201 and 374 bp, respectively. *B*, total RNA was isolated from mouse liver and kidney and reverse-transcribed. Resulting cDNA was amplified with primers annealing in exons 24 and 25. A 329- and a 221-bp fragment was amplified from *Spna2*^{S} and *Spna2*^{R} cDNA, respectively. Each sample shows a similar amount of total RNA. *C*, electrophoregram of the sequenced 221-bp amplicon reveals a correct deletion of the three targeted exons. *D*, liver lysates from different mice were prepared, and proteins (50 μg) were separated by SDS-PAGE on 7% acrylamide gels. Proteins were transferred onto nitrocellulose membrane and hybridized with antibodies specific either for wild-type (*WT*) (*top*), mutant αII-spectrin (*middle*), or with antibodies recognizing both αII-spectrins (*bottom*). This figure is a representation of two independent mice of each genotype.

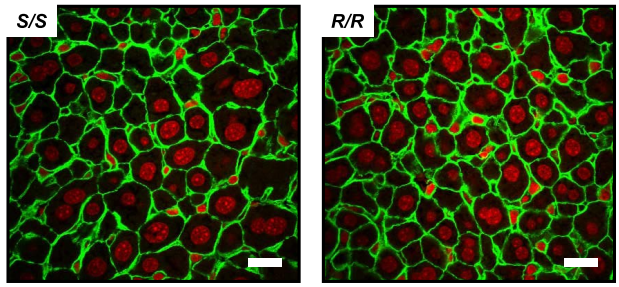

FIGURE 3. **αII-spectrin immunodetection in liver from *S/S* or *R/R* mice.** αII-spectrin (pseudocolored in *green*) was stained with affinity-purified polyclonal antibodies against αII-spectrin SH3 domain on 3-μm tissue sections from the liver of mice. Nuclei were counterstained with propidium iodide (pseudo-colored in *red*). *Scale bar*, 20 μm. No differences were observed between wild-type and mutant liver samples. Similarly, no anomalies have been identified in all others investigated organs (data not shown).

bodies reveal wild-type and mutant spectrins. We did not find any significant variation in the amount of αII-spectrin between the different samples. Thus the mutation we introduced does not alter αII-spectrin expression either at the RNA or at the protein levels.

An extensive histopathological examination of 6-month-old male ($n = 3$) and female ($n = 3$) mutants and wild-type male ($n = 1$) and female ($n = 1$) counterparts failed to detect any significant anomaly in mutant mice (data not shown). Furthermore, no abnormalities were found in several organs (kidney, liver, colon, spleen, and brain) from 18-month-old mice. We assumed that this mutation affects only the fragility of αII-spectrin to proteases and not its ability to be incorporated into membrane skeleton, because all domains responsible for interaction with other molecular partners are presumably kept intact. Therefore, we analyzed the cell location of mutant spectrin in different tissues by immunohistochemistry using antibodies against the SH3 domain. In all organs analyzed (brain, heart, lung, stomach, spleen, duodenum, colon, liver, kidney, and skin), the αII-spectrin distribution was the same regardless of whether it was expressed in wild-type or mutant mice. One example in liver is presented in Fig. 3. We did not find any sign of intracellular accumulation of αII-spectrin.

Our results showed that the specific CCC region of αII-spectrin seems dispensable with regard to mouse reproduction and development. These features could be explained by the use of other cleavage sites by calpains and caspases. So it was important to show unambiguously that the mutant *Spna2*^{R} allele bears the expected properties. We therefore further analyzed the proteolytic pattern of mutant αII-spectrin.

Mutant Spectrin Is Resistant to Proteases in Vitro—In a first approach, αII-spectrin present in Triton-soluble lysates from *S/S* and *R/R* livers was submitted to proteases such as μ-calpain (calpain I), caspase 2, and caspase 3. αII-spectrin is cleaved by the two ubiquitous calpains, called m and μ, which differ by the calcium concentration required for activation (m-calpain is activated by millimolar calcium and μ-calpain by micromolar calcium). As expected, μ-calpain digestion of wild-type spectrin generates a unique N-terminal breakdown product (136 kDa calculated) and two C-terminal breakdown products (Fig. 4*B*, *Cter BDP*). The 150-kDa C-terminal BDP (calculated molecular mass of 149 kDa) arises from the calpain cleavage site at residue Tyr-1176. The cleavage site producing the 145-kDa C-terminal BDP is unknown. In contrast, αII-spectrin in *R/R* lysates is resistant to calpain digestion (Fig. 4*B*).

Caspase 3 is a well characterized protease of the CCC region. It was shown previously that the degradation of αII-spectrin occurs in a two-step mechanism (21). First, caspase 3 cuts in the CCC region behind Asp-1185, generating a 137-kDa N-terminal BDP and a 148-kDa C-terminal BDP. The 148-kDa fragment is further cleaved after the Asp-1478, generating 34- and 114-kDa fragments (often described as the "120-kDa" fragment) as shown in Fig. 4*A*. In our *in vitro* experiments, caspase

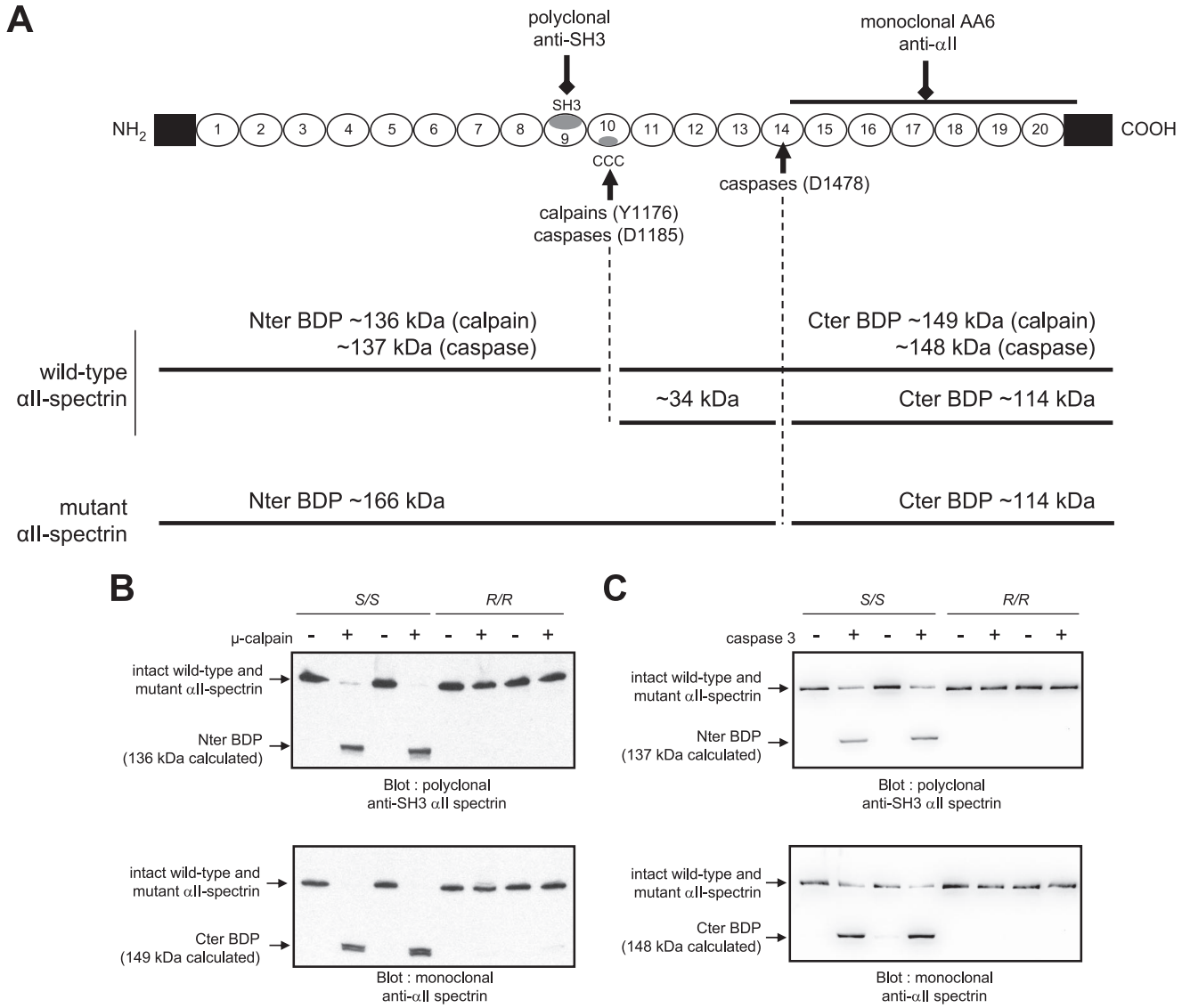

FIGURE 4. **αII-spectrin breakdown in liver lysate from *S/S* and *R/R* mice.** *A,* wild-type αII-spectrin molecule is represented by a succession of triple helical repeats (*ovals with numbers*) and by the nonhomologous N- and C-terminal ends (*black rectangles*). The SH3 domain and the CCC region are also indicated. Depicted are the caspase and calpain cleavage sites (each enzyme cleaves behind the indicated amino acid) in αII-spectrin and the produced breakdown products from each wild-type and mutant αII-spectrins. Both halves of αII-spectrin are revealed as follows: the anti-SH3 antibodies reveal the N-terminal breakdown product because the SH3 domain is upstream of the CCC region. The monoclonal anti-αII-spectrin antibody AA6 reveals the C-terminal fragments (*C-ter BDP*) of αII-spectrin because the epitope is located downstream of the CCC region, in a region included between repetitive units 14 and 21 (21). *B* and *C,* detergent extracts (50 μg) obtained from livers of different mice were subjected to *in vitro* digestion with μ-calpain (*B,* 3.2 units/μl of reaction) with 100 nM calmodulin at 30 °C for 1 h, or with caspase 3 (*C,* 1.5 units/μl of reaction) at 30 °C for 4 h, or were sham-digested without enzyme. After SDS-PAGE (7% acrylamide), Western blots were probed with either polyclonal anti-αII-spectrin SH3 domain (*upper panel*) or monoclonal anti-αII-spectrin (*lower panel*). The size of each breakdown product is indicated. The mutant spectrin is resistant to digestion with caspase or calpain. This figure is a representation of two independent mice of each genotype.

3 cuts wild-type spectrin from Triton-soluble lysates only at the first site and not at the second site as shown in Fig. 4*C* with the detection of the 137- and 148-kDa products revealed by both antibodies. We found that mutant αII-spectrin is completely resistant to caspase 3. Caspase 2 cuts αII-spectrin from wild-type lysate at the same major cleavage site as caspase 3 but not in the second site (11, 21). Mutant αII-spectrin is also completely resistant to caspase 2 (data not shown).

It has been shown that calpains are activated in post-mortem samples (22). So we analyzed the endogenous proteolytic pattern of αII-spectrin prepared from pieces of liver kept at 4 °C during 48 h. This analysis was performed by Western blot on spectrin present in detergent-soluble (Triton) fractions. In *S/S* samples, αII-spectrin is nearly completely cleaved with the presence of one band of 145/150 kDa corresponding to the C-terminal end as detected by monoclonal antibody against αII-spectrin (Fig. 5). This profile resembles those observed with calpain digestion. The 114-kDa C-terminal BDP, which is specific of caspase digestion, is not produced under these conditions. In the *R/R* samples obtained under such conditions, we observed that αII-spectrin is also strongly resistant as indicated by the high amount of native αII-spectrin concomitant with the absence of cleavage product. In *S/R* samples, we found an intermediate pattern of digestion (Fig. 5). Collectively, all these *in*

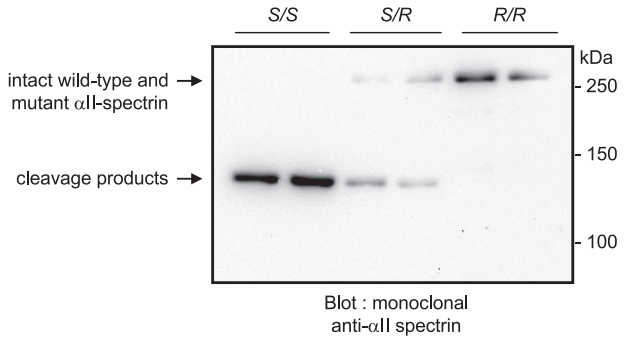

FIGURE 5. **The mutant spectrin is resistant to post-mortem proteolysis.** Pieces of liver were taken from *S/S*, *S/R*, and *R/R* mice and kept at 4 °C for 48 h. Then detergent extracts were prepared (100 μg) and separated by SDS-PAGE (7% acrylamide). Western blot was probed with monoclonal anti-αII-spectrin. This figure is a representation of two independent mice of indicated genotype.

vitro experiments revealed that the mutant αII-spectrin produced by mutant *R/R* mice is strongly resistant to proteolysis.

Analysis of ex Vivo Cleavage—We further analyzed the behavior of mutant spectrin in cultured primary MEF prepared from *S/S* or *R/R* embryos. We observed that $Spna2^{R/R}$ MEFs have a similar behavior than their $Spna2^{S/S}$ counterparts in general growth properties. The morphology of *S/S* or *R/R* MEFs was alike with the presence of stress fibers crossing through the cell and a rim of cortical actin (see examples in Fig. 6, *A* and *B*). Apoptosis was induced in MEFs by UV irradiation. After UV treatment we observed a high proportion of nonadherent cells. Fluorescence-activated cell sorter analysis revealed that they are positive for propidium iodide staining (data not shown) and thus correspond to dead cells. We focused our attention on the status of αII-spectrin cleavage in the population of these dead cells (nonadherent) and the population of still viable (adherent) cells. In contrast to the proteolytic pattern obtained on αII-spectrin presented in cell lysates with exogenous proteases (Fig. 4), αII-spectrin in irradiated dead wild-type and mutant MEFs was completely digested (Fig. 7*A*). The monoclonal anti-αII-spectrin reveals the production of 114-kDa breakdown products demonstrating that caspases can cut at the second site whatever the genotype of αII-spectrin (Fig. 7*A*). When we analyzed the digestion profile using the anti-SH3 antibody, we found the typical 136-kDa breakdown product for αII-spectrin from wild-type dead MEFs. We observed a shift of the size (166 kDa) of the breakdown product for αII-spectrin from mutant MEFs because of the disappearance of the central site and the use of the second site (see Figs. 4*A* and 7*B*). Triton-insoluble fractions produced very similar results with both antibodies (not shown). Thus our experiments showed, as expected, that caspases cannot cleave *ex vivo* in the CCC region and that the secondary site can be used during apoptosis independently of the site present in the CCC region.

The CCC Region Is Not Involved in the Production of Blebs during Apoptosis—It was hypothesized that αII-spectrin cleavage is involved in the blebbing of membrane that occurs during apoptosis. To clarify this point, we triggered apoptosis using UV irradiation in our MEF model, fixed cells, and stained them with anti-αII-spectrin antibody and phalloidin. As shown in Fig. 6 (*C–F*), blebs were present in wild-type

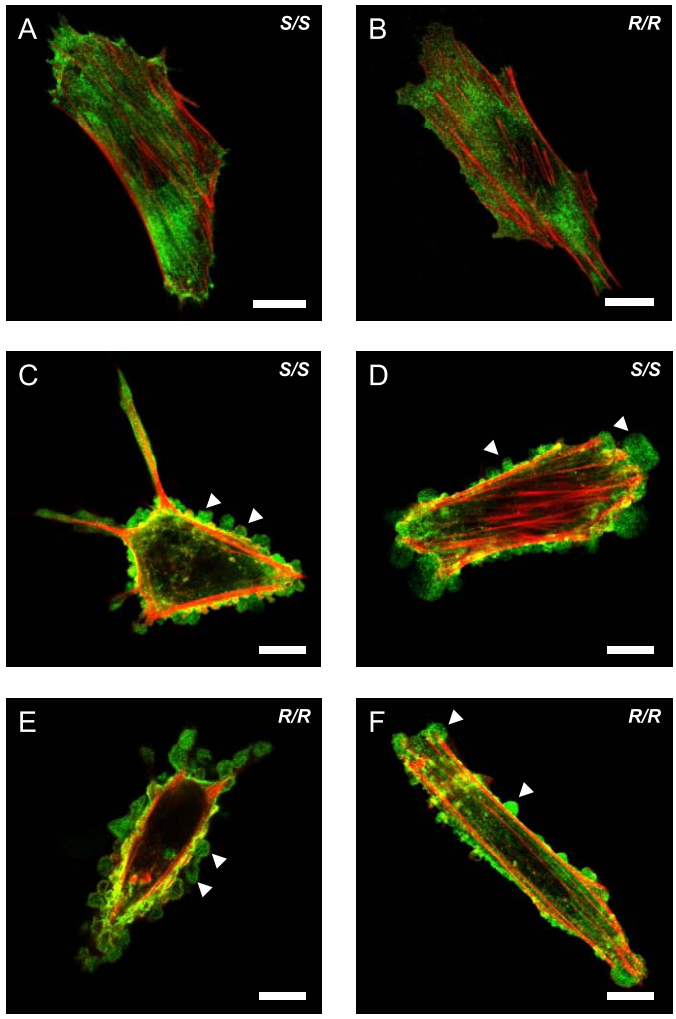

FIGURE 6. **Murine embryonic fibroblasts from *S/S* and *R/R* embryos were cultured and fixed.** The αII-spectrin (pseudocolored in *green*) was stained with affinity-purified polyclonal antibodies against αII-spectrin SH3 domain. Actin (pseudo-colored in *red*) was stained with phalloidin. *S/S* and *R/R* MEFs were untreated (*A* and *B*) or submitted to UV irradiation (*C–F*). Membrane blebbing is indicated with *arrowheads*. *Scale bar*, 20 μm.

MEF as well as in mutant MEF with no noticeable difference between them. This experiment demonstrated that blebbing can occur without any cleavage in the CCC region. Apoptosis triggered by H_2O_2 gave similar results concerning the cleavage profile of mutant αII-spectrin or the production of blebs (data not shown).

Finally, we analyzed the calpain-specific cleavage. We took advantage of the fact that in our culture conditions, αII-spectrin is cut in the CCC region in adherent MEFs when they are freshly spread (30,000 cells/cm^2) on plastic with 10% SVF. We observed two breakdown products with *S/S* MEF of 145 and 150 kDa (Fig. 8*A*). The 150-kDa product probably corresponds to cleavage by caspases, whereas the 145-kDa corresponds to cleavage by calpain. When MEF were incubated with calpain inhibitor ALLN, the lower band is not produced (Fig. 8*B*), indicating that this product is specifically processed by calpains. The *R/R* MEFs produced neither the higher band nor the lower band, again clearly indicating that mutant αII-spectrin is resistant to calpain in *ex vivo* conditions (Fig. 8*B*).

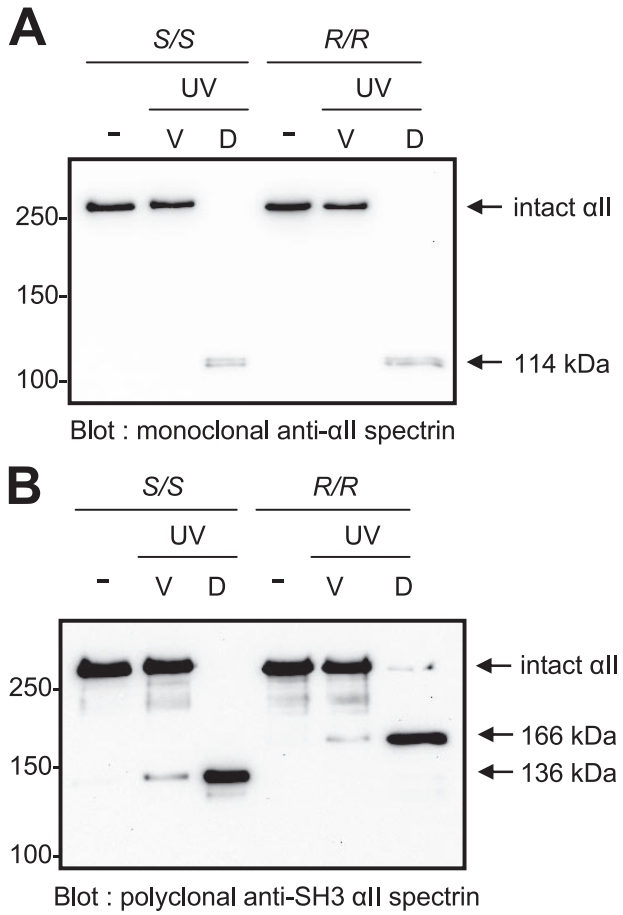

FIGURE 7. **Twenty-four hours after UV treatment, both adherent viable cells (*V*) and nonadherent dead cells (*D*) were harvested separately.** Western blot analysis of the Triton-soluble fractions were performed using either monoclonal anti-αII-spectrin (*A*) or polyclonal anti-αII-spectrin SH3 domain (*B*). The size of each breakdown product (BDP) is indicated.

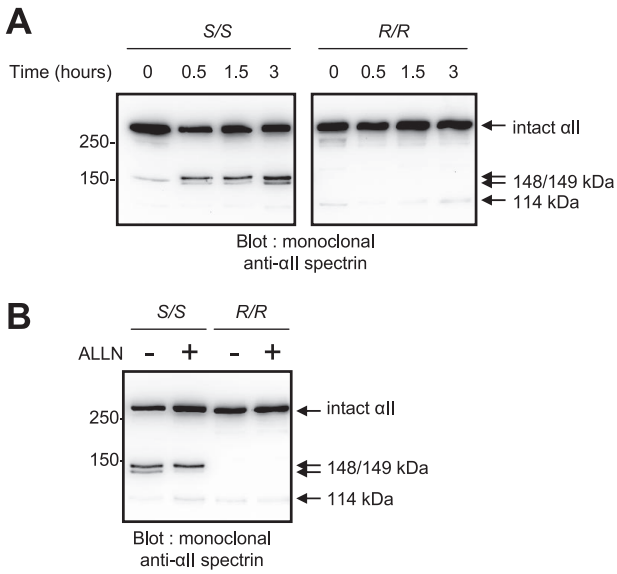

FIGURE 8. *A,* MEFs were plated onto uncoated dishes and cultured for 0.5, 1.5, or 3 h. Cells were harvested, and detergent-soluble lysates were prepared. Western blot analysis was performed using monoclonal anti-αII-spectrin. The size of each breakdown product is indicated. *B,* MEFs were harvested and incubated in new dishes with 5 μM calpain inhibitor ALLN in 0.1% Me_2SO (+) or in 0.1% Me_2SO alone (−) for 3 h. Cells were harvested, and detergent-soluble lysates were prepared. Western blot analysis was performed using monoclonal anti-αII-spectrin. The size of each breakdown product is indicated.

DISCUSSION

Previous genetic studies in *D. melanogaster* and *C. elegans* have demonstrated that mutations in the unique α-spectrin ortholog to the αII-gene of the vertebrates are lethal in larva (8–10), and we assumed that the entire αII-spectrin would also have important functions in vertebrates. Hence, we defined a domain targeting strategy and focused our attention on the specific CCC region, which contains the calpain and caspase cleavage sites as well as the calmodulin binding domain. As indicated by K_a/K_s analysis, this region is highly conserved during the evolution of vertebrates, including in species that diverged several hundred million years ago. We hypothesized that the CCC region bears at least one important function in vertebrates, and we created a murine model specifically lacking the CCC region. It should be noted that this region does not exist in αII-spectrin from invertebrates. Surprisingly, we obtained healthy homozygote mice with a normal cage behavior. Histological and immunohistochemical analysis demonstrated lack of abnormalities at the organ or cellular level and question the importance of αII-spectrin cleavage *in vivo*.

Is αI-spectrin able to compensate the mutant αII-spectrin? This hypothesis is unlikely because the replacement of mutant αII by αI should not lead to the production of an α-spectrin sensitive to cleavage because of the absence of a CCC-like region in αI. Moreover, we did not find any decrease of αII-spectrin expression in tissues from mutant mice. Does an αIII chain exist? This seems unlikely because analysis of the human and the murine genome does not suggest the existence of such a novel spectrin, a possibility that has not been formally excluded. Another compensatory mechanism, if it exists, may involve the cleavage of βII-spectrin, which is also targeted by caspases and calpains (21). Although a high affinity binding site for calmodulin is not present within βII-spectrin, calpain cleavage of βII-spectrin is modulated by the presence of calmodulin (23, 24). The following mechanism has been suggested: after the initial calpain cleavage of αII-spectrin, calmodulin binding on αII-spectrin exposes a calpain-cleavage site on the βII chain, then disrupts the $(\alpha II/\beta II)_2$ spectrin tetramer, and finally down-regulates the binding of αII/βII spectrin to actin (25). Consequently, we expected that removing the principal binding site for calmodulin should have consequences for proteolysis of both chains. We demonstrated that βII-spectrin from mutant lysates can be cleaved *in vitro* by calpains suggesting that the calpain sites of βII are accessible despite the disappearance of the CCC region (data not shown). As a result, the synergy of cleavage between αII and βII is still not clear. Furthermore, a compensatory mechanism via β-chain cannot explain the strong conservation of the CCC region in vertebrates.

We found that the mutant spectrin lost its sensitivity to caspase in its central region. However, the second caspase site is functional *ex vivo,* but we failed to obtain digestion at this site *in vitro*. A simple explanation for the difference between our *in vitro* and *ex vivo* experiments could be that the second site is cleaved by an uncharacterized protease. However, thymocytes derived from caspase 3-deficient mice that underwent apopto-

sis failed to produce cleavage at this second site (26). Alternatively, this protease could be under the control of caspase 3.

In red blood cells, it is well established that a loss of interaction between proteins of membrane skeleton can be associated with blebbing of cells and loss of membrane materials (example in Refs. 27 and 28)). With regard to the similarity between the major components of membrane skeleton from erythroid and nonerythroid cells, it has been proposed that cleavage of spectrin could be responsible for membrane blebbing observed during apoptosis (29, 30). Because we observed normal blebbing in mutant MEFs that underwent apoptosis, we concluded that proteolysis of the CCC region during apoptosis is not an initially required event in this process or that the cleavage at the second site of αII or in βII-spectrin is sufficient for it. Several studies suggested that αII-spectrin is initially cleaved at a caspase 3 consensus site (Asp-1185), and this primary event likely alters the structural conformation of the protein exposing subsequent cleavage sites and altering cytoskeletal integrity (31). However, this is not compatible with our results.

The αI and βI chains that form spectrin tetramers found in red blood cells interact with a lower affinity than αII and βII chains (32). Thus, the erythroid membrane skeleton is probably more flexible than the membrane skeleton found in nonerythroid cells. This physical property could be responsible for the deformability and remarkable stability to shear stress. We assume that specific proteolytic processes exist in αII-spectrin to deform the robust membrane skeleton of cells, *e.g.* during cell differentiation or mitosis. In fact, it was demonstrated that spectrin redistributes to the cytosol during mitosis (33). However, taking into account all our results, we concluded that CCC deletion introduces a change in the proteolytic property of αII-spectrin but clearly had no severe consequences for these mice or cells derived from them. It should be noted that if a partial proteolytic process by caspases is maintained, this is not the case for calpain proteolysis. Thus we argued that the good health of the mutants cannot only be explained simply by the maintenance of the second caspase site, especially as it was demonstrated that the cleavage at this site occurs only when cells are apoptotic.

A function for αII-spectrin cleavage could have been remained unidentified if it concerns the long term potentiation process essential for memory. Previous studies have shown that it is possible to obtain mutant mice with no obvious visible phenotype but a strong perturbation in the learning process, which is difficult to appreciate without specific tests (34). Such a perturbation could exist in our mutant mice because of the following. (i) It has been suggested that calpain cleavage of spectrin could be involved in long term potentiation (35). (ii) A protein factor that inhibits ATP-dependent glutamate accumulation into synaptic vesicles has been purified and has been shown to correspond to αII-spectrin breakdown products. Intact αII-spectrin did not have such an inhibitory property (36). (iii) It has been shown that αII/βII spectrin dimer interacts with NR1a, NR2A, and NR2B subunits of *N*-methyl-D-aspartic acid receptor (37), and αII-spectrin is cleaved under *N*-methyl-D-aspartic acid activation. Thus spectrin cleavage could be involved in specific processes allowing modulation of the glutamatergic synaptic transmission or could act directly on the number of glutamate receptors available in the membranes of synapses by modulating the plasticity of the membrane skeleton (38). A defect in these processes could interfere with learning and memory in our murine model; therefore, this hypothesis on our murine model merits further investigation.

Acknowledgments—We thank Colette Galand for valuable assistance in the targeting construct work; Marco Giovaninni for the PGK-hygromycin cassette; Manoussos Koutsourakis and Abdel Ayadi for the work on ES line establishment and chimera production; Martin Holzenberger for the MeuCre40MH line and for the very careful reading and suggestions for the manuscript; Bernard Grandchamp and Carole Beaumont for providing access to animal facility; Olivier Thibaudeau for the help with paraffin blocks and slides preparation; Laurent Gouya and Bernard Grandchamp for fruitful discussions; Joël Nicolas for its assistance in page make-up and informatics; and Dominique Goossens for the careful revision of the text.

REFERENCES

1. Byers, T. J., and Branton, D. (1985) *Proc. Natl. Acad. Sci. U. S. A.* **82,** 6153–6157
2. Mohandas, N., and An, X. (2006) *Transfus Clin. Biol.* **13,** 29–30
3. Delaunay, J. (2007) *Blood Rev.* **21,** 1–20
4. Ikeda, Y., Dick, K. A., Weatherspoon, M. R., Gincel, D., Armbrust, K. R., Dalton, J. C., Stevanin, G., Durr, A., Zuhlke, C., Burk, K., Clark, H. B., Brice, A., Rothstein, J. D., Schut, L. J., Day, J. W., and Ranum, L. P. (2006) *Nat. Genet.* **38,** 184–190
5. Parkinson, N. J., Olsson, C. L., Hallows, J. L., McKee-Johnson, J., Keogh, B. P., Noben-Trauth, K., Kujawa, S. G., and Tempel, B. L. (2001) *Nat. Genet.* **29,** 61–65
6. Komada, M., and Soriano, P. (2002) *J. Cell Biol.* **156,** 337–348
7. Tang, Y., Katuri, V., Srinivasan, R., Fogt, F., Redman, R., Anand, G., Said, A., Fishbein, T., Zasloff, M., Reddy, E. P., Mishra, B., and Mishra, L. (2005) *Cancer Res.* **65,** 4228–4237
8. Lee, J. K., Coyne, R. S., Dubreuil, R. R., Goldstein, L. S., and Branton, D. (1993) *J. Cell Biol.* **123,** 1797–1809
9. Norman, K. R., and Moerman, D. G. (2002) *J. Cell Biol.* **157,** 665–677
10. Praitis, V., Ciccone, E., and Austin, J. (2005) *Dev. Biol.* **283,** 157–170
11. Rotter, B., Kroviarski, Y., Nicolas, G., Dhermy, D., and Lecomte, M. C. (2004) *Biochem. J.* **378,** 161–168
12. Nicolas, G., Fournier, C. M., Galand, C., Malbert-Colas, L., Bournier, O., Kroviarski, Y., Bourgeois, M., Camonis, J. H., Dhermy, D., Grandchamp, B., and Lecomte, M. C. (2002) *Mol. Cell. Biol.* **22,** 3527–3536
13. Nedrelow, J. H., Cianci, C. D., and Morrow, J. S. (2003) *J. Biol. Chem.* **278,** 7735–7741
14. Canizalez-Roman, A., and Navarro-Garcia, F. (2003) *Mol. Microbiol.* **48,** 947–958
15. Navarro-Garcia, F., Canizalez-Roman, A., Sui, B. Q., Nataro, J. P., and Azamar, Y. (2004) *Infect. Immun.* **72,** 3609–3621
16. Simonovic, M., Zhang, Z., Cianci, C. D., Steitz, T. A., and Morrow, J. S. (2006) *J. Biol. Chem.* **281,** 34333–34340
17. Harwood, S. M., Yaqoob, M. M., and Allen, D. A. (2005) *Ann. Clin. Biochem.* **42,** 415–431
18. Leneuve, P., Colnot, S., Hamard, G., Francis, F., Niwa-Kawakita, M., Giovannini, M., and Holzenberger, M. (2003) *Nucleic Acids Res.* **31,** e21
19. Rubera, I., Poujeol, C., Bertin, G., Hasseine, L., Counillon, L., Poujeol, P., and Tauc, M. (2004) *J. Am. Soc. Nephrol.* **15,** 2050–2056
20. Hedges, S. B. (2002) *Nat. Rev. Genet.* **3,** 838–849
21. Wang, K. K., Posmantur, R., Nath, R., McGinnis, K., Whitton, M., Talanian, R. V., Glantz, S. B., and Morrow, J. S. (1998) *J. Biol. Chem.* **273,** 22490–22497
22. Geddes, J. W., Bondada, V., Tekirian, T. L., Pang, Z., and Siman, R. G. (1995) *Neurobiol. Aging* **16,** 651–660

23. Harris, A. S., Croall, D. E., and Morrow, J. S. (1989) *J. Biol. Chem.* **264,** 17401–17408
24. Leto, T. L., Pleasic, S., Forget, B. G., Benz, E. J., Jr., and Marchesi, V. T. (1989) *J. Biol. Chem.* **264,** 5826–5830
25. Harris, A. S., and Morrow, J. S. (1990) *Proc. Natl. Acad. Sci. U. S. A.* **87,** 3009–3013
26. Zheng, T. S., Schlosser, S. F., Dao, T., Hingorani, R., Crispe, I. N., Boyer, J. L., and Flavell, R. A. (1998) *Proc. Natl. Acad. Sci. U. S. A.* **95,** 13618–13623
27. Chen, H., Khan, A. A., Liu, F., Gilligan, D. M., Peters, L. L., Messick, J., Haschek-Hock, W. M., Li, X., Ostafin, A. E., and Chishti, A. H. (2006) *J. Biol. Chem.* **282,** 4124–4135
28. Peters, L. L., Shivdasani, R. A., Liu, S. C., Hanspal, M., John, K. M., Gonzalez, J. M., Brugnara, C., Gwynn, B., Mohandas, N., Alper, S. L., Orkin, S. H., and Lux, S. E. (1996) *Cell* **86,** 917–927
29. Martin, S. J., O'Brien, G. A., Nishioka, W. K., McGahon, A. J., Mahboubi, A., Saido, T. C., and Green, D. R. (1995) *J. Biol. Chem.* **270,** 6425–6428
30. Lee, A., Morrow, J. S., and Fowler, V. M. (2001) *J. Biol. Chem.* **276,** 20735–20742
31. Williams, S. T., Smith, A. N., Cianci, C. D., Morrow, J. S., and Brown, T. L. (2003) *Apoptosis* **8,** 353–361
32. Bignone, P. A., and Baines, A. J. (2003) *Biochem. J.* **374,** 613–624
33. Fowler, V. M., and Adam, E. J. (1992) *J. Cell Biol.* **119,** 1559–1572
34. Grant, S. G., O'Dell, T. J., Karl, K. A., Stein, P. L., Soriano, P., and Kandel, E. R. (1992) *Science* **258,** 1903–1910
35. Lynch, G., and Baudry, M. (1987) *Brain Res. Bull.* **18,** 809–815
36. Ozkan, E. D., Lee, F. S., and Ueda, T. (1997) *Proc. Natl. Acad. Sci. U. S. A.* **94,** 4137–4142
37. Wechsler, A., and Teichberg, V. I. (1998) *EMBO J.* **17,** 3931–3939
38. Lynch, G., Rex, C. S., and Gall, C. M. (2007) *Neuropharmacology* **52,** 12–23